MRI parameters of Alzheimer's disease in an Arab population of Wadi Ara, Israel

Abdalla Bowirrat[1]
Irith I Reider-Groswasser[2]
Marlene Oscar-Berman[1,3]
Orna Aizenstein[2]
Gad Levy[2]
Amos D Korczyn[4]

[1]Department of Anatomy and Neurobiology, and Division of Psychiatry, Boston University School of Medicine, Boston, ME, USA; [2]Section of Neuroradiology, Department of Imaging, Tel Aviv Sourasky Medical Center, and Sackler Faculty of Medicine, Tel Aviv University, Tel Aviv, Israel; [3]Boston Department of Veterans Affairs Healthcare System and Department of Neurology, Boston University School of Medicine, Boston, ME, USA; [4]Department of Neurology, Tel Aviv Medical Center, and Sieratzki Chair of Neurology, Tel Aviv University, Ramat-Aviv, Israel

Correspondence: Abdalla Bowirrat
Department of Anatomy and Neurobiology, Laboratory of Neuropsychology, Boston University School of Medicine, 715 Albany Street, L-815 Boston, MA 02118, USA
Tel +1 617 638 4807
Fax +1 617 638 4806
Email bowirrat@bu.edu

Abstract: Magnetic resonance imaging (MRI) findings are reported from 15 individuals in an Arab–Israeli community who were diagnosed with Alzheimer's disease (AD). The quantitative parameters that were used for MRI analyses included gradings (0–3) and linear measurements of different brain structures. Generalized tissue loss was assessed by combined measurements of the ventricles (ventricular score, VS) and sulcal grading and width (SG, SW, respectively). Loss of brain tissue in specific regions of interest, eg, temporal lobes, basal ganglia, and midbrain, was evaluated by precise measurements. We observed abnormal tissue characteristics, expressed as high intensity foci in white matter on T2W sequences, as well as tissue loss, both generalized and focal. Most notable were changes involving the head of the caudate nuclei, the midbrain, and to a lesser degree, medial temporal structures.

Keywords: magnetic resonance imaging, linear measures, brain structure, Alzheimer's disease, Arab population, Wadi-Ara, Israel

Introduction

The clinical diagnosis of Alzheimer's disease (AD) remains problematic, as it is largely based on the exclusion of other diseases. In particular, it is difficult to detect AD in its early stages and discriminate it from other similar mental disorders (Winblad et al 1986). Different diagnostic approaches, ie, positron emission tomography (PET), single photon emission computed tomography (SPECT), neuropsychology, neurogenetics, and electrophysiology have not yet provided definitive differential features. Therefore, a reliable diagnostic method is needed for precise diagnosis without invasive techniques (particularly at the onset of AD) (Dickerson et al 2001; Killiany et al 2002; Koga et al 2002; Kantarci and Jack 2003). Structural neuroimaging techniques such as magnetic resonance imaging (MRI) have played an important role in the initial evaluation of dementia, especially for ruling out potentially treatable etiologies. Findings such as ventricular enlargement, prominence of sulci, and cerebral white matter areas of increased T_2-weighted signal intensity on MRI have been correlated with age, dementia of Alzheimer's type, prior stroke, and hypertension (Longstreth et al 1996; Yue et al 1997; Wahlund et al 2001; Hampel et al 2002; Teipel et al 2002; Bronge 2003; de Leeuw et al 2004; Jack et al 2004). Volumetric, planimetric, and simple cross-sectional linear and area measurements of brain structures seem to improve early diagnosis of AD (Frisoni et al 1996; Pucci et al 1996; Dickerson et al 2001; Killiany et al 2002; Koga et al 2002; Kantarci and Jack 2003).

In the present study, we used a simple computerized linear MRI-based method of measurement for evaluating the presence of AD, taking into consideration its reproducibility, accuracy, and efficiency, as well as its excellent intraobserver reliability. In contrast to volumetric measurement methods, which are very time-consuming, the linear MRI method has easy applicability for almost all brain

© 2005 Dove Medical Press Limited. All rights reserved

structures. Additionally, linear-based measures are less constrained than volumetric measures in the assessment of subcortical nuclei and limbic structures, such as the hippocampus and parahippocampal gyrus, because of the anatomical features of these structures (Frisoni et al 1996; Pucci et al 1998; Whalley and Wardlaw 2001).

The Arab–Israeli community of the rural area of Wadi Ara is unique with respect to having high rates of dementia of Alzheimer's type (DAT) (Bowirrat et al 2001, 2002). The high prevalence of DAT in this population was not explained by ApoE-ε4 allele, since this population was found to have the lowest frequency of this allele ever recorded (Bowirrat et al 2000). The ApoE distributions in this small group was as follows: six patients (6/15) were found to carry the ApoE allele (all heterozygous) = ApoE-ε4/ε3, and nine patients (9/15) were found to carry ApoE allele = ApoE-ε3/ε3. Although those patients fulfilled DSM-IV[1] and NINCDS-ADRDA[2] criteria for AD (McKhann et al 1984; APA 1994), autopsy confirmation is lacking, and because of local tradition it is unlikely to become available.

The aim of the present study was to use structural MRI to characterize the brains of patients with AD, using quantitative parameters enabling description of findings in a standardized approach (Reider-Groswasser 1997; Heinik et al 2000; Kantarci and Jack 2003). Linear MRI-based measurements (which correspond to the maximum distance between two end points from side to side) as well as semi-quantitative gradings of the findings in this population are detailed. These data delineate the morphometric characteristics of Wadi Ara AD patients.

Methods

Patient characteristics

In our previous studies (Bowirrat et al 2001, 2002), we identified a high prevalence of DAT among the elderly population of Wadi Ara, Israel. Many individuals had mild cognitive deficits, although they did not fulfill DSM-IV criteria for dementia (APA 1994). In a follow-up study we identified several cases (n = 24) who progressed to become demented. From among these 24 cases, 15 (8 males) were selected for MRI studies. We excluded cases with significant other diseases, such as cancer, severe cardiac disease, and arthritis, because these disorders might either affect the patients' transport or complicate the analysis of the results. The mean age of the 15 cases was 76 years (range 74–78 years). Their mean Mini-Mental State Examination (MMSE) score (Folstein et al 1975) was 16.2 (SD ± 4).

MRI acquisition

The MRI study was conducted by a team of neurologists and radiologists at Tel-Aviv Medical Center, Israel and Boston University Medical School, USA, who arrived at a consensus regarding the MRI findings. The MRI scans were acquired on a GE Signa 1.5 Tesla scanner. Although some patients were restless and often needed sedation, the studies were not performed under generalized anesthesia. Scans that contained movement artifacts were not included. For all patients, at least three sequences were obtained: FLAIR, FSET2, and SET1. Axial slices were obtained parallel to a cut passing through the line connecting the anterior and the posterior commissures (AC-PC line). Their thickness was 3.5 mm, with 1 mm between adjacent cuts. Coronal cuts were perpendicular to the AC-PC line. The thickness of the cuts was 3.0 mm, and the distance between adjacent cuts was 0.8 mm. Sagittal cuts were performed through planes parallel to the midline. Their thickness was 5 mm with a 2 mm gap between adjacent cuts. Field of view for the axial and sagittal cuts was 24 cm × 24 cm and 24 cm × 18 cm, and for the coronal cuts 24 cm × 18 cm.

MRI analyses

The presence of focal lesions in the brain was documented as either hyperintense T2 FLAIR lesions, or infarcts (either cortical or lacunar). The hyperintense T2 signals were graded into subgroups WMG1 (graded from 0 to 9) and WMG2 (graded from 0 to 3) according to procedures described by Manolio et al (1994), Bryan et al (1994), and Longstreth et al (1996) for grading white matter changes (WMG) (graded from 0 to 9) (Table 1).

Regarding the linear measurements and semiquantitative gradings, axial, coronal, and sagittal MRI cuts were employed. Axial cuts, performed with FLAIR sequence, were used for the linear measurements; FSE T2 sequences were used for coronal measurements; and SET1 sagittal cuts were used for the sagittal measurements. The measurements were performed on the films and adjusted to the ruler that appeared on each cut. Twenty-three landmarks for performing the measurements (numbered sequentially by subscripts) are summarized in Table 1 and detailed as follows:

BCD_1. Bicaudate distance. This is the width of the left and right frontal horns including the septum pellucidum, measured on an axial cut showing the lower part of the frontal horns, just in front of the foramen of Monro (Hughes and Gado 1981). This measurement is also included in CVI-2 and VS (see below).

Table 1 List of 23 measurement landmarks with related references. The landmarks are listed alphabetically and denoted sequentially by subscripts.

Abbreviation	Meaning	References
BCD_1	Bicaudate distance	Hughes et al 1981; Reider-Groswasser et al 1993
CCD_2	Anteroposterior diameter of the genu of the corpus callosum	Laissy et al 1993; Reider-Groswasser et al 1997
CCH_3	Corpus callosum height	
$CH\text{-}H.F_4$	Choroidal-hippocampal fissure grading (right, left)	George et al 1990
CMD_5	Cella media distance	Gyldensted et al 1976; Reider-Groswasser et al 1997
$CVI\text{-}2_6$	Cerebroventricular index 2	Hahn et al 1976; Heinik et al 2000
HH_7	Hippocampal height (right, left)	
IPD_8	Interparietal distance	
IUD_9	Interuncal distance	Dahlbeck et al 1991; Heinik et al 2000
$MBW,L\text{-}L_{10}$	Midbrain maximal latero-lateral width	Reider-Groswasser et al 2002
MD_{11}	Midbrain anteroposterior diameter	Raininko et al 1994; Reider-Groswasser et al 1997
$MD\text{-}C_{12}$	Midbrain length at the center	Schrag et al 2000; Warmuth-Metz et al 2001
MDL_{13}	Midbrain length (right, left)	Doraiswamy et al 1992
PD_{14}	Anteroposterior diameter of the pons	Raininko et al 1994; Reider-Groswasser et al 1997
SCD_{15}	Septum-caudate distance	Gyldensted et al 1976; Reider-Groswasser et al 1997
SG_{16}	Sulcal width grading	Furman 2000
SW_{17}	Sulcal width	Gyldensted 1976; Furman 2000
$TH, a\text{-}p_{18}$	Temporal horn, anteroposterior diameter	Heinik et al 2000; Reider-Groswasser et al 2002
$TH, l\text{-}l_{19}$	Temporal horn, latero-lateral diameter (right, left)	
VS_{20}	Ventricular score	Hughes et al 1981; Reider-Groswasser et al 1993
WMG_{21}	White matter changes grading	Manolio et al 1994; Longstreth et al 1996
$3VW_{22}$	Third ventricle width	Reider-Groswasser et al 1997
$4VD_{23}$	Fourth ventricle anteroposterior diameter	Raininko et al 1994; Reider-Groswasser et al 1997

CCD_2. Anteroposterior diameter of the genu of the corpus callosum. This measure was taken from a sagittal cut along a horizontal line passing between the inner maximal concavity of the genu of the corpus callosum to its outer maximal convexity.

CCH_3. Corpus callosum height. This is the height of corpus callosum on a coronal cut passing at the level of the posterior part of the suprasellar cistern and the clivus. The measurement was performed on a cut showing the posterior part of the supracellar cistern, usually one cut behind the one showing the optic chiasm, in the midline, from the upper edge of the septum pellucidum to the highest point of the corpus callosum.

$CH\text{-}H.F_4$. Choroidal-hippocampal fissure grading (right, left). 0 = no enlargement; 1 = mild enlargement (about pencil line width); 2 = moderately enlarged (2–3 mm in antero-posterior width); 3 = width exceeds 3 mm. Grading was performed for the left and the right sides.

CMD_5. Cella media distance. This was measured as the minimal distance between the bodies of the lateral ventricles. It was measured usually at a cut clearly showing the "waist" of the bodies of the lateral ventricles, which is at the second cut above the cut showing the internal cerebral veins. This measurement is included in VS (see below).

$CVI\text{-}2_6$. Cerebroventricular index. This is the BCD divided by the brain's width at the same level.

HH_7. Hippocampal height (right, left). This measurement was performed on a T2 coronal cut (the third cut posterior to the cut on which the basilar artery is seen). The measurement is from the maximal convexity of the lower border of the hippocampus to the lower border of the adjacent temporal horn. To the best of our knowledge, this measurement has not been defined previously.

IPD_8. Interparietal distance. This measurement was performed on the axial cut at the level of the bodies of the lateral ventricles and on the same cut on which CMD was measured. It is measured from outer to outer margins of the brain at its largest parietal distance.

IUD_9. Interuncal distance. This measurement was performed both on axial and coronal planes. The distance was measured between maximal convexities of the unci on the cut in which the optic chiasm was seen in the suprasellar cistern on an axial cut, and on the cut just posterior to the one showing the optic chiasm on the coronal cut.

$MBW, L\text{-}L_{10}$. Midbrain's maximal latero-lateral width. This measurement was performed on an axial cut across the midbrain at its largest width.

MD_{11}. Midbrain's anteroposterior diameter. This was measured on the sagittal plane along a line drawn from the

highest point of the pons to the posterior end of the tectum between the superior and inferior colliculi. The distance is from the intersection of this line with the midbrain to the posterior end on the tectum.

MD-C_{12}. Midbrain length at the center. This measurement was performed on an axial cut at the center of the midbrain from the most posterior point of the interpeduncular cistern to the posterior border on the tectum in the center.

MDL_{13}. Midbrain length (right, left). This measurement was performed on an axial cut from the center of the posterior border of the tectum along a line passing laterally to the aqueduct of Sylvius to a point intersecting with the crus cerebri on the left and on the right.

PD_{14}. Anteroposterior diameter of the pons. The measurement was performed on the midsagittal cut along a line that passes between the maximal convexity of the pons to the fastigium. The posterior border of the pons is at the intersection of this line.

SCD_{15}. Septum-caudate distance. This was measured on an axial cut from the maximal convexity of the head of the caudate to the medial and anterior border of the frontal horn on the left and the right sides.

SG_{16}. Sulcal width grading. A scale from 0 to 3 was used to measure enlargement of sulci: 0 = no enlargement; 1 = mild enlargement; 2 = moderately enlarged sulci (when four or more sulci are widened above the ventricles, and when there is widening of the interhemispheric fissure in its anterior part); and 3 = severe enlargement (widening of the entire hemispheric fissure).

SW_{17}. Sulcal width. This is the mean value of the sum of the four largest sulci measured at a high convexity cut (typically the third cut above the ventricular bodies).

TH, a-p_{18}. Temporal horn, anteroposterior diameter. This measure was performed on an axial plane on the cut which shows the optic chiasm in the suprasellar cistern. It is measured from the maximal convexity of the posterior border along a straight line to the anterior border of the horn. This measurement was performed for the left and the right sides.

TH, l-l_{19}. Temporal horn, latero-lateral diameter (right, left). This measurement was performed on the coronal view on the cut suitable for the measurement of CCH. This cut is usually just one cut posterior to the cut showing the optic chiasm. The measurement was performed along a horizontal line passing at the largest latero-lateral width of the temporal horns.

VS_{20}. Ventricular score. This is a calculated value, which is the sum of SCD on the left and on the right sides, the BCD, the third ventricle, and the CMD divided by the widest width of the brain on the cut showing the lateral ventricles, IPD.

WMG_{21}. White matter changes grading. Grades ranged from 0 to 9 as suggested by Manolio (1994) and Longstreth (1996): 0 = no white matter changes; 1 = discontinuous periventricular rim with minimal dots of subcortical disease; 2 = thin, continuous periventricular rim with a few patches of subcortical disease; 3 = thicker, continuous periventricular rim with scattered patches of subcortical disease; 4 = thicker, shaggier periventricular rim with mild subcortical disease, and may have minimal confluent periventricular lesions; 5 = mild periventricular confluence surrounding the frontal and occipital horns; 6 = moderate periventricular confluence surrounding the frontal and occipital horns; 7 = periventricular confluence with moderate involvement of the centrum semiovale; and 8 = periventricular confluence

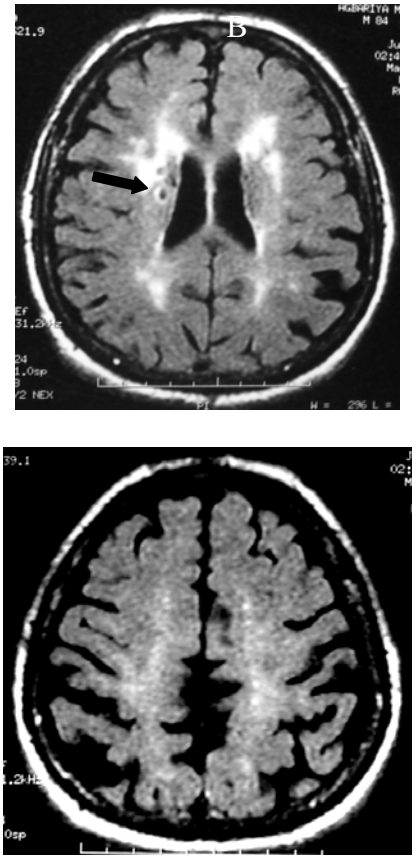

Figure 1 An 80-year-old male with dementia of the Alzheimer's type. Axial flair cut showing hyperintense signal and lacunar infarcts (black arrow) in the periventricular white matter. Grading of white matter changes according to Manolio et al (1994) and Longstreth et al (1996) –8/9.

involving most of the centrum semiovale. Cases with findings more remarkable than grade 8 were scored 9.

$3VW_{22}$. Third ventricle width. This was measured at the axial cut best showing the third ventricle. The width was measured at the junction of middle and posterior thirds of the ventricle.

$4VD_{23}$. Fourth ventricle anteroposterior diameter. This was measured on the midsagittal cut along the line on which the PD was measured. 4VD is the distance from the anterior border of this line to the fastigium.

Results

All 15 patients had hyperintense T2 and FLAIR signals in the white matter, mainly adjacent to the lateral ventricles (Figure 1). Lacunar infarcts were found in 4/15 (26%) of the patients. Cortical infarcts were found only in 1/15 patients (6.5%) (Figures 1 and 2).

Correlations between the sizes of various structures, and their p-values (when significant), are detailed in Table 2. Table 2 shows correlation coefficients (r) obtained for the linear measures of specific brain structures (with significant p-values). Significant correlations were found between the following pairs of measures: the heights of the right and the left hippocampus (Rt HH–Lt HH); the cerebroventricular index 2 and bicaudate distance (CVI-2–BCD); the right temporal horn and left (as well as right) hippocampus (Rt TH–Lt HH, and Rt TH–Rt HH); the right and left temporal horns, in anterior-posterior and in latero-lateral dimensions (Rt TH–Lt TH, in all directions); and midbrain lengths at its center and anterioposterior locations (MD-C–MD).

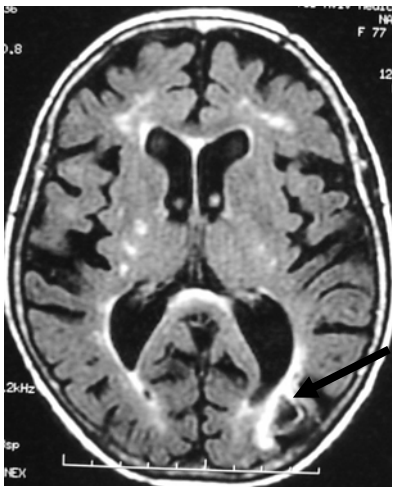

Figure 2 A 77-year-old woman with dementia of the Alzheimer type. Axial flair cut showing hyperintense foci and a small cortical infarct in the left posterior parietal lobe (black arrow). Note the widening of the left occipital horn.

Table 2 Brain structures and correlation coefficient (r) and significant p-values

Brain structures	Correlation coefficient (r) and significant p-value	
	r	p
3VW – CCH	−0.45	
3VW – CCD	−0.51	
PD – CCH	0.5	
CVI-2 – CCH	−0.64	
Rt HH – Lt HH	0.82	0.01
Rt HH – Rt TH	−0.56	
CVI-2 – BCD	0.95	0.006
IUD – CCH	−0.5	
Rt TH, a-p – Lt HH	0.78	0.001
Rt TH, a-p – Rt HH	0.9	0.0008
Rt TH, a-p – Lt TH, a-p	0.96	0.005
Rt TH, a-p – Lt TH l-l	0.55	0.01
MD-C– MD	0.75	0.002
SW-SG	0.65	

Abbreviations: Rt, right; Lt, left; see text for brain structures.

Tables 3, 4, and 5 show linear measurements in millimeters performed on axial, coronal, and sagittal MRI cuts, respectively. The measures indicate generalized tissue loss in the AD patients, as reflected by ventricular score (VS), cerebroventricular index 2 (CVI-2), and ventricle widths (3VW and 4VW). Additionally, midbrain lengths (MDL) on the right and left sides were small, as were bicaudate measures (BCD). Additionally, there was a gender difference in bicaudate distance (BCD), with females showing significantly smaller values than males ($p < 0.03$) (Table 3).

Table 3 Linear measurements in mm, performed on axial MRI cuts

Imaging parameter	Mean	SD
Lt SCD	9.2	1.7
Rt SCD	8.8	2.3
BCD[a]	20.3	3.1
3VW	8.1	1.4
CMD	30.1	5.8
IPD	125.7	4.1
VS	61	9.8
CVI-2	17.8	2.6
IUD	27.5	3.8
Lt TH a-p	5.1	3.1
Rt TH a-p	6.3	5.4
Lt MDL	26	2.3
Rt MDL	26.1	2.2
MD-W	34.1	3.2
MD-C	16.6	2.5
SW	5.1	1.7

[a] BCD, female and male mean values: 18.5 and 21.8, respectively, $p < 0.03$.
Abbreviations: MRI, magnetic resonance imaging; see text for imaging parameters.

Table 4 Linear measurements in mm, performed on coronal MRI cuts

Imaging parameter	Mean	SD
HH Lt	7.4	0.9
HH Rt	7.4	1.2
TH, I-I, Lt	5.2	2.0
TH, I-I, Rt	5.5	5.2
CCH	3.4	0.5

Table 5 Linear measurements in mm, performed on sagittal MRI cuts

Imaging parameter	Mean	SD
MD	16.1	2.5
PD	21.7	2.7
4VD	11.2	0. 9
CCD	10.6	3.2

Discussion

The present study, which involves a group of unique AD patients, is mainly descriptive. We used a simple linear MRI-based measurement method for evaluating brain changes accompanying AD in an elderly Arab population in Israel. Because our results are derived from a small sample size of 15 patients, the utility of linear measurements cannot be assessed completely. Nonetheless, our findings confirm the usefulness of this straightforward and quick approach for characterizing patterns of tissue loss in dementia. Additionally, results of our study are in an agreement with the findings previously reported by Brinkman et al (1981), Wood and Bigler (1995), and Heinik and colleagues (2000) indicating generalized brain tissue loss (reflected by increased ventricular size and sulcal width), hyperintense foci in the white matter changes (mainly periventricular), and the involvement of the caudate nuclei and midbrain.

The basal ganglia – including the caudate nucleus – are known to be affected by neurological disorders such as Parkinson's disease, progressive supranuclear palsy, Huntington's disease, and traumatic brain injury (Cummings 1990; Reider-Groswasser 1997; Heinik et al 2000). Additionally, the caudate plays an important role in cognition, and caudate pathology has been shown to adversely affect cognitive abilities (Cummings 1990; Heinik et al 2000). Involvement of the basal ganglia, including the caudate nucleus, in AD patients was especially convincing in a study by Snowdon et al (1997). The principal aim of that study was to determine the relationship of brain infarction to the clinical expression of AD. Of 102 participants who later died, 61 met the neuropathologic criteria of AD. At autopsy, lacunar infarcts (1.5 cm and larger), senile plaques, and neurofibrillary tangles were seen (Snowdon et al 1997). Fifteen of the patients had one or two lacunar infarcts in the basal ganglia, thalamus, or deep white matter. These findings suggest that cerebrovascular disease may play an important role in determining the presence and severity of the clinical symptoms of AD.

Of interest, we observed significant differences between the genders in the size of bicaudate distance (BCD) (Table 3). Whether this finding is related to the degenerative brain process or to normal differences between genders cannot be elucidated from this study, since we did not scan normal age-matched controls. However, the significant changes involve selective parameters only, and further clarification would be valuable in future studies.

Imaging of the brain for delineation of tissue loss and structural changes, and for the assessment of its function and metabolic alterations, is widely used in patients with dementia (Englund et al 1988; Aliev et al 2002; Bronge 2002; Hogervorst et al 2002; Bronge and Wahlund 2003). Additionally, the studies of Jack et al (2003, 2004) open a new opportunity for the use of volumetric and segmentation techniques as valuable methods for evaluating disease progression as well as the efficacy of clinical trials. In cases where patients cannot be adequately sedated for more complicated studies, however, the simplicity of linear measurements may contribute to diagnostic accuracy and enable repeated measurement and reassessments of parameters in an easy fashion. Here, we successfully used linear measurements for characterizing patterns of tissue loss in AD.

In the present study, positive correlations were found between white matter changes as reflected by corpus callosum parameters (CCH, CCD) and some of the other parameters (Table 2). A lack of statistical significance for these correlations may be attributed to the small size of the group examined. Even so, the positive findings support those of Hampel et al (2002), who reported on corpus callosum atrophy in AD patients and stressed that mainly the splenium and the body of the corpus callosum were affected. The presence of white matter changes in an elderly population in general, and in AD in particular as seen in our study, is also evident from other studies (Englund et al 1988; Tanabe et al 1997; Bronge 2002; Hampel et al 2002; Hogervorst et al 2002; Koga et al 2002; Bronge and Wahlund 2003; de Leeuw et al 2004). The pathogenesis of these changes is probably multifactorial and poorly understood, and recent studies using diffusion tensor imaging suggest that it may be secondary to Wallerian degeneration of fiber tracts due

to neuronal loss in cortical association areas (Bozalli et al 2002; Hampel et al 2002). The vascular abnormalities in AD could reflect on the pathogenesis of the disease and be related to ApoE status (Matsubayashi et al 1992; Kuller et al 1998; Shi et al 2000; Bronge 2002; Korczyn and Chapman 2003). However, our AD group is peculiar because of having marked white matter changes and practically no ApoE-ε4 haplotypes (Bowirrat at el 2000). In these cases, oxidative stress and perfusion injury may underlie the white matter lesions (Aliev et al 2002; Eckert et al 2003; Barnham et al 2004). These findings may indicate that, in fact, several subjects actually suffer from mixed dementia rather than pure AD (Korczyn 2002). The importance of the white matter changes as factors that induce cognitive changes has been stressed in the volumetric MRI study of Koga et al (2002).

The generalized tissue loss in our patients is reflected by ventricular score (VS) and cerebroventricular index 2 (CVI-2) (means of 61% and 17.8%, respectively). The findings are close to the values documented on a computerized tomography (CT) scan study of patients with AD with a mean age of 78 years (means of 62.99% and 17.6%) (Heinik et al 2000) (Tables 1, 3). These close results reflect on the high validity and good reproducibility of the measurements. Also, the significant correlation ($r = 0.75$) between the measurements of the midbrain performed on axial and sagittal planes (MD-C and MD) reflect the accuracy of the measures. The good correlation between grading and measurements (sulcal grade and sulcal width, $r = 0.65$) confirms the usefulness of a semiquantitative approach for standardized imaging studies. This was also found in a previous study assessing tissue loss in patients with post-traumatic head injury (Reider-Groswasser et al 2002).

The medial temporal tissue loss as reflected by the interuncal distance (IUD) is also very close to the values reported by Heinik et al (2000). It is 27.87 mm in the study of Heinik et al (2000) and 27.47 (SD ± 3.8) in our present MRI study (Table 3). The bicaudate distance (BCD) and the CVI-2 correlated significantly with the clock drawing test in the study of Heinik et al (2000), and since the CVI-2 values are so close in both studies, 17.6 (SD ± 3.0) and 17.8 (SD ± 2.6) respectively (as mentioned above, Table 3), it supports the likelihood of caudate involvement in the AD population of Wadi Ara.

The correlations of medial temporal tissue loss (Table 2) reflect their association (TH, HH, IUD). Significant p-values were only seen between the TH on the left and on the right ($p = 0.005$), and between their axial and coronal measures ($p = 0.001$). The correlation between hippocampal height (HH) and temporal horn (TH) as shown in Table 2 also were statistically significant ($p < 0.001$), and should be further assessed in larger series. These results show the usefulness of HH as a parameter for assessment of medial temporal structures. Our data also confirm the major morphologic changes in medial temporal parameters that have been described by others to occur in the course of AD (Frisoni et al 1996; Jack et al 2004).

In the present study, the mean value of the antero-posterior diameter of the midbrain as measured in the axial plane, midbrain length-center (MD-C), is close to the measurement that was performed on the sagittal plane – midbrain anteroposterior diameter (MD) (16.64 and 16.12 mm, respectively) (Tables 3, 5). The decreased midbrain diameter on the axial planes has been described in progressive supranuclear palsy (Schrag et al 2000; Warmuth-Metz et al 2001), and to the best of our knowledge, it has not yet been described in AD. This parameter should be correlated with clinical findings and reassessed in a larger AD population.

Conclusions

In the present study, we used a simple linear MRI-based measurements method for evaluating 15 patients with DAT in an elderly Arab population in Israel. We found altered tissue characteristics, expressed as high intensity foci in white matter on T2W sequences, and tissue loss, both generalized and local (involving the head of the caudate, the midbrain, and to a lesser degree medial temporal structures). The significance of our findings, as well as the additional information derived from correlations among the different parameters, suggest that these patients are a unique group with distinct imaging features, perhaps related to their low frequency of ApoE-ε4 allele. Whatever the underlying mechanisms, results of these investigative analyses warrant consideration in other populations of elderly people. Such patterns may provide clues about the pathophysiology of structural brain changes in the elderly.

Acknowledgments

The research was supported in part by grants from the National Institute of Aging (UO1-AG17173), the National Institute on Alcohol Abuse and Alcoholism (R37-AA07112 and K05-AA00219), and the US Department of Veterans Affairs. We also thank Mr B Lumiansky for technical assistance.

Notes

[1] DSM-IV, Diagnostic and statistic manual of mental disorders, 4th edition.

[2] NINCDS-ADRDA, The National Institute of Neurological Disorders and Stroke, and Association International pour la Recherche et l'Enseignement en Neurosciences.

References

Aliev G, Smith MA, Seyidova D, et al. 2002. The role of oxidative stress in pathophysiology of cerebrovascular lesions in Alzheimer's disease. *Brain Pathol*, 12:21–35.

[APA] American Psychiatric Association. 1994. Diagnostic and statistical manual of mental disorders. Fourth edition (DSM-IV). Washington: APA.

Barnham KJ, Masters CL, Bush AI. 2004. Neurodegenerative diseases and oxidative stress. *Nat Rev Drug Discov*, 3:205–14.

Bowirrat A, Friedland RP, Chapman J, et al. 2000. The very high prevalence of AD in an Arab population is not explained by APOE epsilon4 allele frequency. *Neurology*, 55:731.

Bowirrat A, Friedland RP, Farrer L, et al. 2002. Genetic and environmental risk factors for Alzheimer's disease in Israeli Arabs. *J Mol Neurosci*, 19:239–45.

Bowirrat A, Treves TA, Friedland RP, et al. 2001. Prevalence of Alzheimer's type dementia in an elderly Arab population. *Eur Neurol*, 8:119–23.

Bozalli M, Falini A, Franceschi M, et al. 2002. White matter damage in Alzheimer's disease assessed in vivo using diffusion tensor magnetic resonance imaging. *J Neurol Neurosurg Psychiatry*, 72:742–6.

Brinkman SD, Sarwar M, Levin HS, et al. 1981. Quantitative indexes of computed tomography in dementia and normal aging. *Radiology*, 138:89–92.

Bronge L. 2002. Magnetic resonance imaging in dementia: a study of brain white matter changes. *Acta Radiol Suppl*, 428:1–32.

Bronge L, Wahlund LO. 2003. Prognostic significance of white matter changes in a memory clinic population. *Psychiatry Res Neuroimaging*, 122:199–206.

Bryan RN, Manolio TA, Schertz LD, et al. 1994. A method for using MR to evaluate the effects of cardiovascular disease on the brain: the cardiovascular health study. *Am J Neuroradiol*, 15:1625–33.

Cummings JL (ed). 1990. Subcortical dementia. New York: Oxford University Pr.

Dahlbeck JW, McCluney KW, Yeakley JW, et al. 1991. The interuncal distance: a new MR measurement for the hippocampal atrophy in Alzheimer's disease. *Am J Neuroradiol*, 12:931–2.

de Leeuw FE, Barkhof F, Scheltens P. 2004. White matter lesions and hippocampal atrophy in Alzheimer's disease. *Neurology*, 62:310–12.

Dickerson BC, Goncharova I, Sullivan MP, et al. 2001. MRI-derived entorhinal and hippocampal atrophy in incipient and very mild Alzheimer's disease. *Neurobiol Aging*, 22:747–54.

Doraiswamy PM, Na C, Husain MM, et al. 1992. Morphometric changes of the human midbrain with normal aging: MR and stereologic findings. *AJNR Am J Neuroradiol*, 13:383–6.

Eckert A, Marques C, Keil U, et al. 2003. Increased apoptotic cell death in sporadic and genetic Alzheimer's disease. *Ann N Y Acad Sci*, 1010: 604–9.

Englund E, Brun A, Alling C. 1988. White matter changes in dementia of Alzheimer's type. Biochemical and neuropathological correlates. *Brain*, 111(Pt 6):1425–39.

Folstein MF, Folstein SE, McHugh PR, et al. 1975. Mini-Mental State. A practical method for grading the cognitive state of patients for clinician. *J Psychiatr Res*, 12:189–98.

Frisoni GB, Beltramello A, Weiss C, et al. 1996. Linear measures of atrophy in mild Alzheimer disease. *AJNR*, 17:913–23.

Furman M. 2000. Comparison between computed tomography findings in patients with infarcts in vascular territories of middle and posterior cerebral artery. MD thesis presented to Hadassa Medical School, Jerusalem, 2000. Available from The Hebrew University, Jerusalem, Israel.

George AE, deLeon MJ, Stylopoulus LA, et al. 1990. CT diagnostic features of Alzheimer's disease: importance of the choroidal hippocampal fissure complex. *AJNR Am J Neuroradiol*, 11:101–7.

Gyldensted C, Kosteljanetz M. 1976. Measurements of the normal ventricular system with computer tomography: a preliminary study on 44 adults. *Neuroradiology*, 10:205–13.

Hahn FJ, Rim K. 1976. Frontal ventricular dimensions on normal computed tomography. *Am J Roentgenol*, 126:593–6.

Hampel H, Teipel SJ, Alexander GE, et al. 2002. In vivo imaging of region and cell type specific neocortical neurodegeneration in Alzheimer's disease. Perspectives of MRI derived corpus callosum measurement for mapping disease progression and effects of therapy. Evidence from studies with MRI, EEG and PET. *J Neural Transm*, 109:837–55.

Heinik J, Reider-Groswasser II, Solomesh I, et al. 2000. Clock drawing test: correlation with linear measurements of CT studies in demented patients. *Int J Geriatr Psychiatry*, 15:1130–7.

Hogervorst E, Mendes Ribeiro H, Molyneux A, et al. 2002. Plasma homocysteine levels, cerebrovascular risk factors, and cerebral white matter changes (leukoaraiosis) in patients with Alzheimer disease. *Arch Neurol*, 59:787–93.

Hughes CP, Gado M. 1981. Computed tomography and aging of the brain. *Radiology*, 139:391–6.

Jack CR Jr, Shiung MM, Gunter JL, et al. 2004. Comparison of different MRI brain atrophy rate measures with clinical disease progression in AD. *Neurology*, 62:591–600.

Jack CR Jr, Slomkowski M, Gracon S, et al. 2003. MRI as a biomarker of disease progression in a therapeutic trial of milameline for AD. *Neurology*, 60:253–60.

Kantarci K, Jack CR Jr. 2003. Neuroimaging in Alzheimer disease: an evidence-based review. *Neuroimaging Clin N Am*, 13:197–209.

Killiany RJ, Hyman BT, Gopmez-Isla T, et al. 2002. MRI measures of entorhinal cortex vs hippocampus in preclinical AD. *Neurology*, 58:1188–96.

Koga H, Yuzuriha T, Yao H, et al. 2002. Quantitative MRI finding and cognitive impairment among community dwelling elderly subjects. *J Neurol Neurosurg Psychiatry*, 72:737–41.

Korczyn AD. 2002. Mixed dementia – the most common cause of dementia. *Ann N Y Acad Sci*, 977:129–34.

Korczyn AD, Chapman J. 2003. Apolipoprotein E, dementia and strokes. *J Neurol Sci*, 206:3–5.

Kuller LH, Shemanski L, Manolio T, et al. 1998. Relationship between ApoE, MRI findings, and cognitive function in the cardiovascular health study. *Stroke*, 29:388–98.

Laissy JP, Patrux B, Duchateau C, et al. 1993. Midsagittal MR measurements of the corpus callosum in healthy subjects and diseased patients: a prospective survey. *AJNR Am J Neuroradiol*, 14:145–54.

Longstreth WT Jr, Manolio TA, Arnold A, et al. 1996. Clinical correlates of white matter findings on cranial magnetic resonance imaging of 3301 elderly people. The Cardiovascular Health Study. *Stroke*, 27:1274–82.

Manolio TA, Kronmal RA, Burke GL, et al. 1994. Magnetic resonance abnormalities and cardiovascular disease in older adults. The Cardiovascular Health Study. *Stroke*, 25:318–27.

Matsubayashi K, Shimada K, Kawamoto A, et al. 1992. Incidental brain lesions on magnetic resonance imaging and neurobehavioral functions in the apparently healthy elderly. *Stroke*, 23:175–80.

McKhann G, Drachman DA, Folstein M, et al. 1984. Clinical diagnosis of Alzheimer disease report of the NINDS-ADRDA work Group. *Neurology*, 34:939–44.

Pucci E, Belardinelli N, Regnicolo L, et al. 1998. Hippocampus and parahippocampal gyrus linear measurements based on magnetic resonance in Alzheimer's disease. *Eur Neurol*, 39:16–25.

Raininko R, Autti T, Vanhanen SL, et al. 1994. The normal brain stem from infancy to old age. A morphometric MRI study. *Neuroradiology*, 36:364–8.

Reider-Groswasser I, Cohen M, Costeff H, et al. 1993. Late CT findings in brain trauma: relationship to cognitive and behavioural sequelae and to vocational outcome. *AJR*, 160:147–52.

Reider-Groswasser I, Costeff H, Sazbon L, et al. 1997. CT findings in persistent vegetative state following blunt traumatic brain injury. *Brain Inj*, 11:865–70.

Reider-Groswasser II, Groswasser Z, Ommaya AK, et al. 2002. Quantitative imaging in late traumatic brain injury. Part I: late imaging parameters in closed and penetrating head injuries. *Brain Inj*, 16:517–25.

Reider-Groswasser I, Ommaya AK, Salazar AM, et al. 1997. Neuroimaging assessment in TBI and stroke: relevance for acute and post acute treatment. In Leon-Carrion J, ed. Neuropsychological rehabilitation: fundamental, directions and innovations. Florida: GR/St Lucie Pr. p 73–108.

Schrag A, Good CD, Miszkiel K, et al. 2000. Differentiation of atypical Parkinsonian syndromes with routine MRI. *Neurology*, 54:697–702.

Shi J, Perry G, Smith MA, et al. 2000. Vascular abnormalities: the insidious pathogenesis of Alzheimer's disease. *Neurobiol Aging*, 21:357–61.

Snowdon DA, Greiner LH, Mortimer JA, et al. 1997. Brain infarction and the clinical expression of Alzheimer disease – The Nun Study. *JAMA*, 277:813–17.

Tanabe JL, Amend D, Schuff N, et al. 1997. Tissue segmentation of the brain in Alzheimer disease. *Am J Neuroradiol*, 18:115–23.

Teipel SJ, Bayer W, Alexander GE, et al. 2002. Progression of corpus callosum atrophy in Alzheimer's disease. *Arch Neurol*, 59:243–8.

Wahlund LO, Barkhof F, Fazekas F, et al. 2001. A new rating scale for age-related white matter changes applicable to MRI and CT. *Stroke*, 32:1318–22.

Warmuth-Metz M, Naumann M, Csoti I, et al. 2001. Measurement of the midbrain diameter on routine magnetic resonance imaging: a simple and accurate method of differentiating between Parkinson disease and progressive supranuclear palsy. *Arch Neurol*, 58:1076–9.

Whalley HC, Wardlaw JM. 2001. Accuracy and reproducibility of simple cross-sectional linear and area measurements of brain structures and their comparison with volume measurements. *Neuroradiology*, 43: 263–71.

Winblad B, Fowler CJ, Marcusson J. 1986. Critique of antemortem markers of Alzheimer's disease. *Neurobiol Aging*, 7:388–9.

Wood DMG, Bigler ED. 1995. Diencephalic changes in traumatic brain injury: relationship to sensory perceptual function. *Brain Res Bull*, 18:545–9.

Yue NC, Arnold AM, Longstreth WT Jr, et al. 1997. Sulcal, ventricular, and white matter changes at MR imaging in the aging brain: data from the cardiovascular health study. *Radiology*, 202:33–9.